THE JOURNAL OF PHYSICAL CHEMISTRY A

ARTICLE

pubs.acs.org/JPCA

Vibrational Energy Relaxation in Liquid HCl and DCl via the Linearized Semiclassical Method: Electrostriction versus Quantum Delocalization

Francisco X. Vázquez, Surma Talapatra, and Eitan Geva*

Department of Chemistry, University of Michigan, Ann Arbor, Michigan 48109-1055, United States

ABSTRACT:

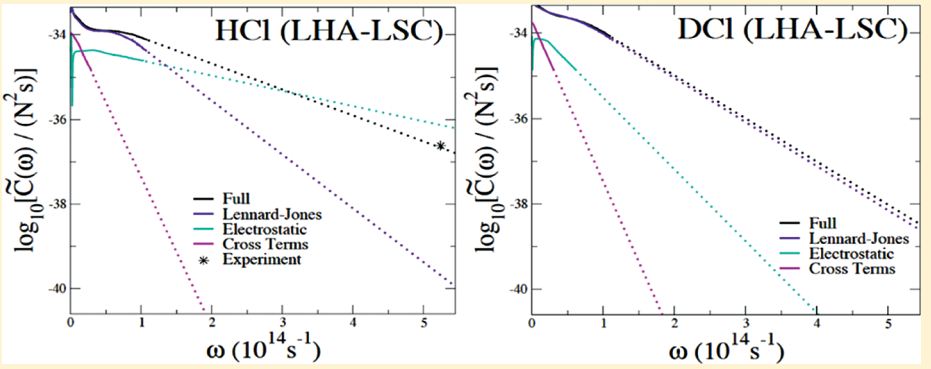

The rate constant for vibrational energy relaxation of the H−Cl stretch in liquid HCl (T = 188K, ρ = 19.671 nm^{-3}) is calculated within the framework of the Landau−Teller formula. The force−force correlation function is calculated via the recently introduced force-derivative-free linearized semiclassical method [Vázquez et al. *J. Phys. Chem. A* **2010**, *114*, 5682]. The calculated vibrational energy relaxation rate constant is found to be in excellent agreement with experiment, and the electrostatic force is found to contribute significantly to the high frequency component of the force−force correlation function. In contrast, the corresponding *classical* vibrational energy relaxation rate constant is found to be 2 orders of magnitude slower than the experimental value, and the classical force−force correlation function is found to be dominated by the Lennard-Jones forces. These observations suggest that quantum delocalization, enhanced by the light mass of hydrogen, amplifies the contribution of repulsive Coulombic forces to the force−force correlation function, thereby making electrostriction an unlikely mechanism for vibrational energy relaxation in the case of hydrogen stretches. This interpretation is reinforced by the results of a similar calculation in the case of the D−Cl stretch in liquid DCl under the same conditions. In this case, the quantum enhancement of the vibrational energy relaxation rate constant is observed to be greatly diminished in comparison to HCl, thereby giving rise to a reversal of the isotope effect in comparison to that predicted by the corresponding classical treatment (i.e., whereas the classical vibrational energy relaxation rate of DCl is faster than that of HCl, the opposite trend is predicted by the linearized semiclassical treatment). It is also shown that the vibrational energy relaxation of DCl is completely dominated by the Lennard-Jones forces within either classical and semiclassical treatments, thereby suggesting that electrostriction is the underlying mechanism in this case.

I. INTRODUCTION

Virtually all chemical phenomena involve vibrational energy relaxation (VER) processes. As a result, the measurement and calculation of VER rates have received much attention over the past few decades.[1−46] Recent theoretical and computational studies of VER have been mostly based on the Landau−Teller (LT) formula,[15,47,48] which gives the VER rate constant in terms of the Fourier transform (FT), at the vibrational transition frequency, of the quantum-mechanical autocorrelation function of the fluctuating force exerted on the relaxing mode by the other degrees of freedom (DOF), i.e., the bath.

Importantly, replacing the quantum-mechanical force−force correlation function (FFCF) by its classical counterpart can only be justified in cases where the vibrational transition frequency is significantly smaller than $k_BT/\hbar$.[49−53] In a series of recent papers,[54−59] we have pursued a rigorous approach for calculating VER rate constants ,which can account for quantum effects within the framework of the linearized semiclassical (LSC) approximation. This approximation amounts to linearizing the forward−backward action in the exact path-integral expression for the quantum-mechanical FFCF with respect to the difference between the forward and backward paths.[60] The resulting expression for the VER rate constant within the LSC approximation involves a Wigner transform[61] of the form $(\exp[-\beta\hat{H}]\hat{F})_W(\mathbf{Q},\mathbf{P})$, where $\beta = 1/k_BT$, $\hat{H}$ is the bath Hamiltonian operator, $\hat{F}$ is the bath-induced force operator, and $(\mathbf{Q},\mathbf{P})$ are the classical-like

Received: April 8, 2011
Revised: July 15, 2011
Published: July 19, 2011

bath positions and momenta. The calculation of this Wigner transform is highly challenging in the case of a many-body anharmonic system like a molecular liquid. Thus, in practice, we have calculated it by employing a local harmonic approximation (LHA), which amounted to calculating the FT underlying the Wigner transform within the instantaneous normal mode approximation. Importantly, our implementation of the LHA only affects the sampling of bath initial momenta while the sampling of bath initial positions is still done in a quantum-mechanically exact manner via imaginary-time path-integral simulations,[62,63] which are based on the exact anharmonic force-fields.

The applicability and reliability of the resulting LHA−LSC method have been previously demonstrated on a variety of nonpolar systems, including liquid O_2,[55,56] liquid N_2,[55,56] O_2/Ar liquid mixtures,[56] H_2 dissolved in liquid Ar,[59] and CX_2 (X = O, S, Se) dissolved on liquid Ar and Ne.[57,58] However, extending the range of applicability to more complex systems has proven cumbersome due to the fact that calculating the standard FFCF within LHA−LSC requires force derivatives as input. In an effort to overcome this obstacle, we have recently introduced a new force-derivative-free computational scheme for calculating VER rate constants within LHA−LSC.[64] The new scheme is based on applying the LSC approximation to the symmetrized FFCF. Unlike the previous scheme[60] which was based on applying LSC to the standard FFCF, the new scheme does not involve a power expansion of the initial force in terms of the Wigner transform integration variable $\mathbf{\Delta}$ and as a result is more accurate and does not require force derivatives as input (for more details, see section II).[64] In ref 64, we tested the new scheme by using it to calculate VER rates in the case of liquid O_2 and liquid N_2 and comparing them to the experimental rates as well as the rates obtained within the original scheme. Avoiding the calculation of force derivatives would be particularly advantageous in applications to more complex systems governed by various types of force fields. In this paper, we take a first step in this direction by presenting the first ever application of the LHA−LSC method to a polar liquid.

VER rates in polar solutions have received much attention over the past several decades. The central role played by electrostatic interactions in enhancing VER rates has already been demonstrated in early measurements performed on neat heteronuclear diatomic liquids.[65−67] For example, the VER lifetime for neat liquid HCl, which is a few nanoseconds long,[66] becomes as long as 1.3 μs when HCl is diluted in a nonpolar solvent such as Xenon.[26] A related class of systems that received much attention corresponds to molecular ions in polar solvents. For example, the VER lifetime of CN^- infinitely diluted in aqueous solution was found to be as short as ∼30 ps.[20,41]

The wealth of detailed experimental information on VER in polar liquid solutions has motivated many theoretical studies that have attempted to provide a molecular interpretation of the VER rate enhancement.[42,45,68−81] However, most of those theoretical studies were based on classical molecular dynamics (MD) simulations, although a few have also attempted to account for quantum-mechanical effects by using quantum corrections factors (QCFs).[42,75,82] The first computational study of VER in a polar solution was carried out by Whitnell et al. on CH_3Cl (treated as an effective diatom with a frequency of ∼680 cm^{-1}) in water.[68,69] The calculated VER lifetime of 5 ps, as obtained from either nonequilibrium classical MD simulations or via the LT formula, is similar to the experimentally observed VER rates in polar solutions. It was also found that the calculated VER rate decreased by at least 1 order of magnitude in the absence of electrostatic interactions, which is consistent with the view that strong electrostatic interactions can significantly enhance the VER rate. Similar classical calculations of VER rates were performed on many other systems, including I_2^- in water and ethanol,[70] a hydrogen bonded complex (A−H···B) in an aprotic dipolar liquid,[71] HgI in ethanol,[72] OClO in water,[73] HOD in D_2O,[42,74,75] CN^- in water,[78] azide in water,[76,77] neat liquid chloroform,[45] neat liquid methanol,[79,80] and HF in water.[81]

Several different arguments have been invoked for explaining the enhancement of VER rates in polar solutions. For example, in the case of aqueous solutions, it appears that the VER rate acceleration is at least partially due to the high density of states in the (700−800) cm^{-1} frequency range, which is attributed to collective librational modes. This leads to rapid VER in cases where the frequency of the relaxing mode overlaps this range (e.g., in the case of CH_3Cl).[68,69] At the same time, the enhanced VER rate in the case of I_2^- in water is believed to be due to the significantly lower vibrational frequency of I_2^- (in comparison to I_2), rather than the stronger solute−solvent interactions.[70,83,84] However, such arguments cannot explain the relatively rapid VER rates in a system such as liquid HCl where VER presumably occurs by energy exchange between a high-frequency H−Cl stretch (2783 cm^{-1}) and a multitude of low-frequency rotational and translational accepting modes. Ladanyi and Stratt have argued, based on classical MD simulations involving a dipolar solute in aprotic polar solvents, that the enhancement of the VER rate by electrostatic forces in such cases can be attributed to a phenomenon they referred to as electrostriction.[85] More specifically, the attractive Coulombic forces bring the solute and solvent closer together, thereby amplifying the effect of non-Coulombic short-range repulsive forces. The fact that these repulsive forces sharply vary can then lead to a rather dramatic enhancement of the VER rate.

As mentioned above, treating VER within the framework of classical mechanics is reasonable in cases such as I_2^- and HgI, where $\beta\hbar\omega \leq 1$. Indeed, the VER lifetime of 1.3 ps measured for I_2^- in water[27] compares relatively well with the 0.6 ps lifetime predicted from classical simulations.[70] The same is true in the case of HgI in ethanol, where the experimental VER lifetime of 3 ps[29] compares well with the classical prediction of 2 ps.[72] However, for the intermediate frequency molecule ClO^- (∼ 700 cm^{-1}), one starts observing significant deviations between the measured VER lifetime of 1−7 ps[86] and the classical predictions of 0.2−0.6 ps.[86,83] The reliability of the classical treatment becomes even more questionable in cases such as HCl and CN^-, where $\beta\hbar\omega \gg 1$. Furthermore, our previous work has shown that a major contribution to the quantum enhancement of the VER rate in nonpolar solutions comes from the fact that quantum delocalization allows the system to sample regions of configuration space where the repulsive forces are stronger.[54−56] At the same time, classical MD simulations suggest that the enhancement of the VER rate by electrostatic forces results from electrostriction, which also leads to enhanced sampling in regions of configuration space where nonelectrostatic repulsive forces are stronger.[83,85] Thus, our goal in this paper is to elucidate the intriguing interplay between quantum delocalization and electrostriction in the case of liquid HCl, which has been chosen because of its high frequency (2783 cm^{-1}) and the fact that experimental VER rates are available for it.[66]

The remainder of this paper is organized as follows. The force-derivative-free LHA−LSC method is briefly outlined in section II. The model for liquid HCl and simulation techniques are outlined in section III. The results are reported and discussed in section IV. The main conclusions are summarized in section V.

II. THE FORCE-DERIVATIVE-FREE LHA−LSC METHOD

In this section we provide a brief outline of the force-derivative-free LHA−LSC method (see ref 64 for a more detailed discussion). To this end, we consider the following general quantum-mechanical Hamiltonian of a vibrational mode linearly coupled to a bath:

$$\hat{H}_{\mathrm{tot}} = \frac{\hat{p}^2}{2\mu} + v(\hat{q}) + \sum_{j=1}^{N} \frac{(\hat{P}^{(j)})^2}{2M^{(j)}} + V(\hat{\mathbf{Q}}) - \hat{q}F(\hat{\mathbf{Q}}) \quad (1)$$

Here, $\hat{q}$, $\hat{p}$, μ, and $v(\hat{q})$ are the relaxing mode coordinate, momentum, reduced mass, and bath-free vibrational potential; $\hat{\mathbf{Q}}$, $\hat{\mathbf{P}}$, $\{M^{(1)}, ..., M^{(N)}\}$, and $V(\hat{\mathbf{Q}})$ are the coordinates, momenta, masses, and potential energy of the bath DOF; and $F(\hat{\mathbf{Q}})$ is the potential force exerted by the bath on the relaxing mode.

The LT formula for the population relaxation rate constant between the first-excited and ground vibrational states can then be given by the following expression:[64]

$$k_{10} = \frac{1}{2\mu\hbar\omega_{10}} e^{\beta\hbar\omega_{10}/2} \tilde{C}_s(\omega_{10}) \quad (2)$$

Here, ω_{10} is the transition frequency and

$$\tilde{C}_s(\omega) = \int_{-\infty}^{\infty} dt e^{i\omega t} C_s(t) \quad (3)$$

is the FT of the *symmetrized* quantum-mechanical FFCF

$$C_s(t) = \frac{1}{Z} Tr[e^{-\beta\hat{H}/2}\delta\hat{F}e^{-\beta\hat{H}/2}e^{i\hat{H}t/\hbar}\delta\hat{F}e^{-i\hat{H}t/\hbar}] \quad (4)$$

where $\hat{H} = \Sigma_{j=1}^{N} [(\hat{p}^{(j)})^2/2M^{(j)}] + V(\hat{\mathbf{Q}})$ is the bath Hamiltonian, $Z = \mathrm{Tr}(e^{-\beta\hat{H}})$ is the canonical bath partition function, and $\delta\hat{F} = \hat{F} - \mathrm{Tr}[e-\beta\hat{H}\hat{F}]/Z$. We also note that in the classical limit, $e^{\beta\hbar\omega_{10}/2}\tilde{C}_s(\omega_{10})$ reduces into the FT of the classical FFCF, $\tilde{C}^{\mathrm{Cl}}(\omega_{10})$, so that eq 2 reduces into

$$k_{10}^{\mathrm{Cl}} = \frac{1}{2\mu\hbar\omega_{10}} \tilde{C}^{\mathrm{Cl}}(\omega_{10}) \quad (5)$$

The LSC approximation for $C_s(t)$ is given by[54,64]

$$C_s^{\mathrm{LSC}}(t) = \frac{1}{(2\pi\hbar)^N} \frac{1}{Z} \int d\mathbf{Q}_0 \int d\mathbf{P}_0 [e^{-\beta\hat{H}/2}\delta\hat{F}e^{-\beta\hat{H}/2}]_W(\mathbf{Q}_0, \mathbf{P}_0)\delta F(\mathbf{Q}_t^{\mathrm{Cl}}) \quad (6)$$

where $\mathbf{Q}_t^{\mathrm{Cl}}$ is obtained by classical dynamics with $\mathbf{Q}_0$ and $\mathbf{P}_0$ as the initial conditions. It should be noted that the LSC approximation only accounts for quantum effects in the initial sampling and not the subsequent dynamics. The accuracy of the LSC approximation, despite its inability to account for the quantum nature of the underlying dynamics, is attributed to the fact that the high-frequency FT of the FFCF is dominated by the short time behavior of the correlation function, which is in turn dominated by the initial sampling.

The main challenge in calculating $C_s^{\mathrm{LSC}}(t)$ lies in evaluating the following Wigner transform:

$$[e^{-\beta\hat{H}/2}\delta\hat{F}e^{-\beta\hat{H}/2}]_W(\mathbf{Q}_0, \mathbf{P}_0) = \int d\Delta e^{-iP_0\Delta/\hbar} \left\langle \mathbf{Q}_0 + \frac{\Delta}{2} \middle| e^{-\beta\hat{H}/2}\delta\hat{F}e^{-\beta\hat{H}/2} \middle| \mathbf{Q}_0 - \frac{\Delta}{2} \right\rangle \quad (7)$$

Evaluating the latter within the LHA as shown in ref 64 leads to the following LHA−LSC approximation for $C_s(t)$:

$$C_s^{\mathrm{LHA-LSC}}(t) = \int d\mathbf{Q}_0 \int d\mathbf{Q}' \frac{\langle \mathbf{Q}_0|e^{-\beta\hat{H}/2}|\mathbf{Q}'\rangle\langle\mathbf{Q}'|e^{-\beta\hat{H}/2}|\mathbf{Q}_0\rangle}{Z} \int d\mathbf{P}_n \prod_{j=1}^{N} \left(\frac{1}{\alpha^{(j)}\pi\hbar^2}\right)^{1/2} \exp\left[-\frac{(P_n^{(j)})^2}{\hbar^2\alpha^{(j)}}\right] \times \delta F(\mathbf{Q}')\delta F(\mathbf{Q}_t^{\mathrm{Cl}}[\mathbf{Q}_0, \mathbf{P}_0]) \quad (8)$$

Here, $\mathbf{P}_n = \mathbf{P}_n(\mathbf{Q}')$ are the normal mode momenta that emerge from diagonalizing the Hessian matrix underlying the quadratic expansion of the bath potential energy around $\mathbf{Q} = \mathbf{Q}'$ and

$$\alpha^{(j)} = \alpha^{(j)}(\mathbf{Q}') = \frac{\Omega^{(j)}(\mathbf{Q}')}{\hbar} \coth\left[\frac{\beta\hbar\Omega^{(j)}(\mathbf{Q}')}{2}\right] \quad (9)$$

where $\{(\Omega^{(k)})^2(\mathbf{Q}')\}$ are the eigenvalues of the Hessian matrix.

It should be noted that unlike the original LHA−LSC scheme for calculating the FFCF,[55] calculating eq 8 does not require force derivatives as input. It should also be noted that eq 8 reduces to the classical FFCF in the classical limit and that nonclassical behavior of the symmetrized FFCF is accounted for in several ways:

1. Nonclassical sampling of bath coordinates and momenta.
2. The initial force, $\delta F(\mathbf{Q}')$, is not calculated at the initial position, $\mathbf{Q}_0$, used to generate the classical trajectory leading to the force at a later time t, $\delta F(\mathbf{Q}_t^{\mathrm{Cl}}[\mathbf{Q}_0, \mathbf{P}_0])$.
3 The factor $e^{\beta\hbar\omega_{10}/2}$, which actually coincides with the so-called Schofield QCF.[87]

III. MODEL PARAMETERS AND SIMULATION TECHNIQUES

The calculations of $C_s^{\mathrm{LHA-LSC}}(t)$ reported below were based on eq 8 and carried out following the algorithm outlined below:

1. Perform an imaginary-time path integral molecular-dynamics (PIMD) simulation[62,63] in order to sample the initial configuration, $\mathbf{Q}_0$, and the configuration at which the initial force is calculated, $\mathbf{Q}'$. To this end, it should be noted that within the context of a PIMD simulation, each DOF is represented by a cyclic polymer of P beads labeled 0, 1, 2, ..., $P-1$. Assuming that P is even, $\mathbf{Q}_0$ is identified with the configuration of the beads labeled 0, while $\mathbf{Q}'$ is identified with the configuration of the beads labeled $P/2$.
2. Perform an LHA around $\mathbf{Q}'$, find the normal-mode frequencies, $\{\Omega^{(k)}\}$, and corresponding transformation matrix, $\{T_{l,k}\}$, and use it to calculate $\{\alpha^{(k)}\}$ and sample the initial (normal-mode) momenta, $\{P_n^{(k)}\}$.
3. Calculate $\mathbf{Q}_t^{\mathrm{Cl}}$ via a classical MD simulation for each sampled initial configuration $\mathbf{Q}_0$ and normal mode momenta $\mathbf{P}_{n,0}$, and time correlate $\delta F(\mathbf{Q}_t^{\mathrm{Cl}})$ with $\delta F(\mathbf{Q}')$.

dx.doi.org/10.1021/jp203302a | J. Phys. Chem. A 2011, 115, 9775–9781

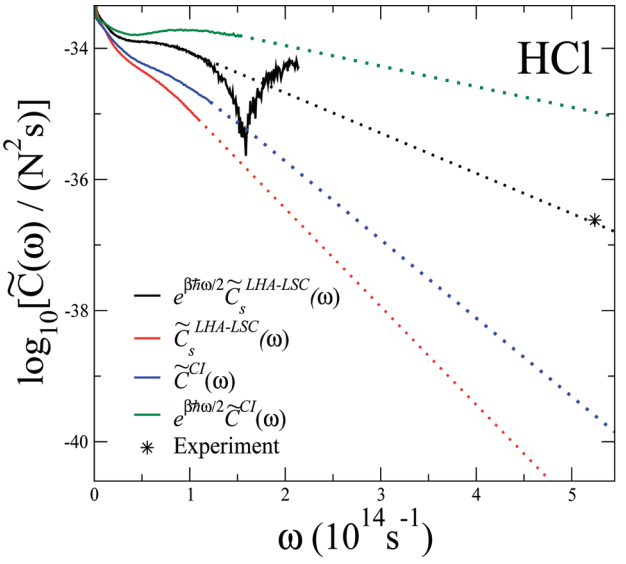

Figure 1. A semilog plot of $e^{\beta\hbar\omega/2}\tilde{C}_s^{LHA-LSC}(\omega)$, $\tilde{C}_s^{LHA-LSC}(\omega)$, $\tilde{C}^{Cl}(\omega)$ and $e^{\beta\hbar\omega/2}\tilde{C}^{Cl}(\omega)$ (Schofield QCF) for neat liquid HCl (T = 188 K, ρ = 19.671 nm^{-3}). Solid lines were obtained from calculations, and dashed lines correspond to extrapolations. The star corresponds to the experimental value at the transition frequency.

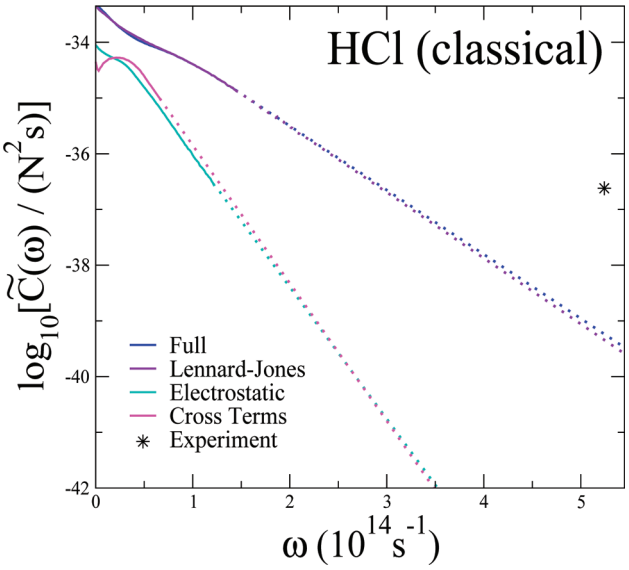

Figure 2. A semilog plot of the LJ−LJ, electrostatic−electrostatic, and LJ−electrostatic cross term contributions to $\tilde{C}^{Cl}(\omega)$ for neat HCl (T = 188 K, ρ = 19.671 nm^{-3}).

Table 1. k_{10}/ns^{-1} for Neat Liquid HCl and DCl at 188K[a]

	$k_{0\leftarrow1}$ (HCl)/ns^{-1}	$k_{0\leftarrow1}$ (DCl)/ns^{-1}	$k_{0\leftarrow1}$(HCl)/$k_{0\leftarrow1}$(DCl)
experiment	1.3		
LHA−LSC	1.3 ± 0.9	0.7 ± 0.3	2 ± 1
classical	0.055 ± 0.009	0.06 ± 0.01	0.9 ± 0.2
Schofield QCF	(14 ± 4) × 10	8 ± 1	17 ± 6

[a] The experimental result for HCl was adopted from ref 66.

4. Repeat steps 1−3 and average over the results until reaching the desired convergence.

Simulations were performed on a liquid consisting of rigid HCl molecules. Energy relaxation via resonant vibrational energy transfer between HCl molecules, as opposed to nonresonant energy relaxation via transfer of vibrational energy into nonvibrational DOF (i.e., translations and rotations), is not considered because it does not affect the ensemble-averaged vibrational energy. More specifically, if one HCl molecule transfers its excess vibrational energy to another HCl molecule, the overall ensemble-averaged vibrational energy does not change, whereas transferring it to nonvibrational DOF clearly decreases the ensemble-averaged vibrational energy. Intermolecular interactions were modeled in terms of Lennard-Jones (LJ) and electrostatic site−site pair interactions. LJ parameters were adopted from the general AMBER force field (GAFF),[88] and partial charges were assigned using a HF/6-31G* restrained electrostatic potential (RESP) and were given by $\delta_H = -\delta_{Cl} = 0.171593e$.The quantum mechanical calculations were done using Gaussian 03. Calculations were preformed using the AMBER molecular dynamics software package on a liquid at 188 K, with a density of 19.671 nm^{-3}, for which the experimental VER rate constant is available.[66] All calculations were preformed with 500 molecules contained in a cubic cell with periodic boundary conditions. PIMD simulations were preformed with 32 beads per atom. Each FFCF was averaged over 180 000 trajectories, each of length 4 ps.

In the absence of resonance with other vibrations, $\tilde{C}_s(\omega)$ was observed to decay asymptotically with frequency in an exponential manner. As a result, it becomes increasingly more difficult to average out the statistical noise accompanying any real-life simulation that is needed in order to calculate the increasingly small value of $\tilde{C}_s(\omega)$ at high frequencies. The results reported below were obtained by following the common practice of obtaining $\tilde{C}_s(\omega)$ at high frequencies by extrapolating the exponential gap law, which emerged at significantly lower frequencies.[89−91] It should be noted that, strictly speaking, the exponential gap law has only been rigorously derived in the case of exponential repulsion interaction.[90] However, it was observed to be valid for the system under discussion in this paper.

IV. RESULTS AND DISCUSSION

In Figure 1, we compare $e^{\beta\hbar\omega/2}\tilde{C}_s^{LHA-LSC}(\omega)$ and $\tilde{C}_s^{LHA-LSC}(\omega)$, as obtained via eq 8, with the corresponding classical $\tilde{C}^{Cl}(\omega)$ and $e^{\beta\hbar\omega/2}\tilde{C}^{Cl}(\omega)$. The corresponding predictions for the VER rate constants are shown in Table 1. The VER rate constant obtained from LHA−LSC via eq 8 is in excellent agreement with the experimental result. At the same time, the corresponding classical VER rate is 2 orders of magnitude slower than the experimental result, which is consistent with the expectation of strong quantum effects in a system that involves a transition frequency that is about 20 times larger than $k_BT/\hbar$. It should also be noted that $\tilde{C}_s^{LHA-LSC}(\omega) < \tilde{C}^{Cl}(\omega)$ throughout the entire range of frequencies. Thus, the combined effect of nonclassical initial sampling and the fact that the initial force is calculated at $\mathbf{Q}'$, rather than at $\mathbf{Q}_0$, is to *diminish* the value of $\tilde{C}_s^{LHA-LSC}(\omega)$ relative to its classical counterpart. However, it should be remembered that a more meaningful comparison is between $\tilde{C}^{Cl}(\omega)$ and $e^{\beta\hbar\omega/2}\tilde{C}_s^{LHA-LSC}(\omega)$. Indeed, $e^{\beta\hbar\omega/2}\tilde{C}_s^{LHA-LSC}(\omega)$ is significantly larger than $\tilde{C}^{Cl}(\omega)$, and more so with increasing frequency. Finally, it should also be noted that applying the Schofield QCF to the classical

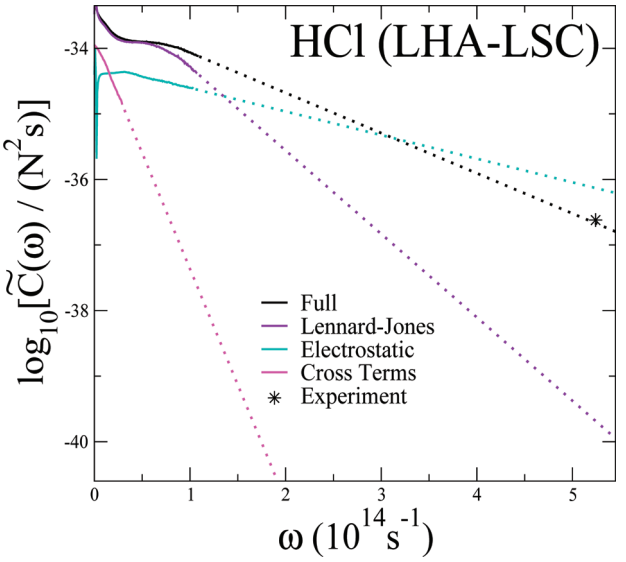

Figure 3. A semilog plot of the LJ−LJ, electrostatic−electrostatic, and LJ−electrostatic cross term contributions to $e^{\beta\hbar\omega/2}\tilde{C}_s^{LSC-LHA}(\omega)$ for neat HCl (T = 188 K, ρ = 19.671 nm^{-3}).

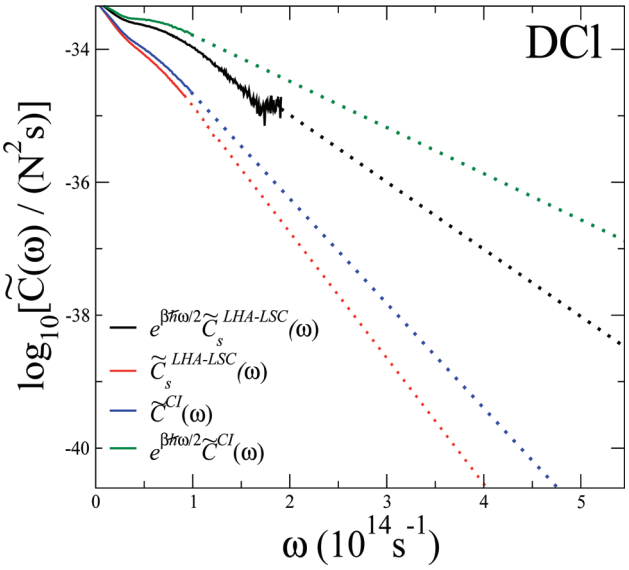

Figure 4. A semilog plot of $e^{\beta\hbar\omega/2}\tilde{C}_s^{LHA-LSC}(\omega)$, $\tilde{C}_s^{LHA-LSC}(\omega)$, $\tilde{C}^{Cl}(\omega)$, and $e^{\beta\hbar\omega/2}\tilde{C}^{Cl}(\omega)$ (Schofield QCF) for neat liquid DCl (T = 188 K, ρ = 19.671 nm^{-3}). Solid lines were obtained from calculations, and dashed lines correspond to extrapolations.

result, i.e., $e^{\beta\hbar\omega/2}\tilde{C}^{Cl}(\omega)$, leads to an overestimation of the VER rate constant by a factor of ∼50 (see Figure 2).

In order to gain insight into the role played by electrostatic forces in determining the VER rate in this system, we decomposed the force into its LJ and electrostatic contributions and considered the LJ−LJ, electrostatic−electrostatic, and LJ−electrostatic cross terms contributions to the FFCF. In Figure 2, we compare these individual contributions in the classical case. The results clearly show that $\tilde{C}^{Cl}(\omega)$ is completely dominated by the nonpolar LJ−LJ contribution, which is consistent with the view that the electrostatic forces only play an indirect role through electrostriction, by allowing the liquid to access otherwise forbidden regions higher on the LJ repulsive walls.

In Figure 3, we compare the LJ−LJ, electrostatic−electrostatic, and LJ−electrostatic cross term contributions to $e^{\beta\hbar\omega/2}\tilde{C}_s^{LSC-LHA}(\omega)$. Similarly to the classical case, we find that the LJ and electrostatic forces are uncorrelated and that, as a result, the cross terms do not contribute significantly to the VER rate. However, in contrast to the classical case, the electrostatic−electrostatic term is seen to make a significant contribution to the VER rate so that the LHA−LSC VER rate constant is no longer dominated by the LJ−LJ term. In fact, by extrapolation, it appears that the relative contribution of the electrostatic-electrostatic term becomes increasingly more dominant with increasing frequency. This result is surprising in light of the fact that the classical treatment points to electrostriction as the mechanism underlying VER in this system. Instead, we find that at least within the LHA−LSC treatment, the FT of the electrostatic−electrostatic FFCF decays more slowly with frequency, thereby making its contribution to the VER rate constant more important with increasing frequency. The origin for this qualitatively different behavior may be traced back to the fact that quantum delocalization allows the system to access nonclassical regions of configuration space where the electrostatic repulsive forces between the hydrogens are larger than in the classical case. Thus, instead of electrostriction where the attractive Coulombic forces bring the solute and solvent closer together, thereby

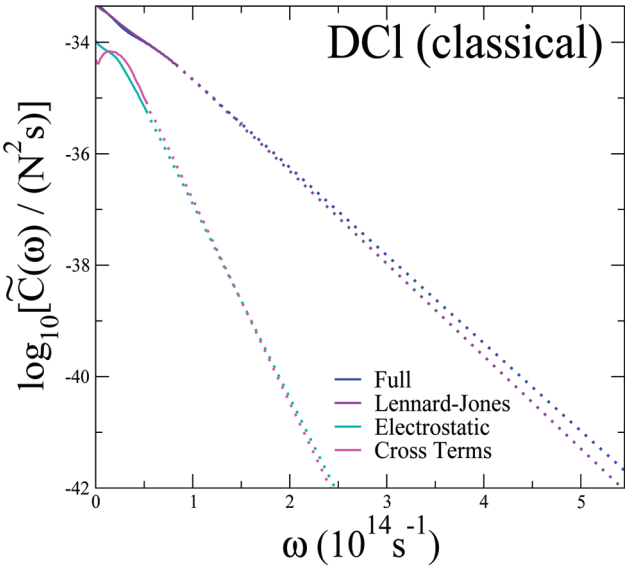

Figure 5. A semilog plot of the LJ−LJ, electrostatic−electrostatic, and LJ−electrostatic cross term contributions to $\tilde{C}^{Cl}(\omega)$ for neat DCl (T = 188 K, ρ = 19.671 nm^{-3}).

amplifying the effect of non-Coulombic short-range repulsive forces, quantum delocalization brings the hydrogens closer than they would have been classically, thereby amplifying the contribution of repulsive Coulombic forces to the VER rate.

Further support for this interpretation comes from a similar calculation of the VER rate constant in the case of DCl (see Table 1 and Figures 4−6). The substitution of the hydrogen by the heavier deuterium is seen to manifest itself by a dramatically smaller quantum enhancement (by less than a factor of 4 as opposed to 2 orders of magnitude). This results in trend reversal in the dependence of the VER rate constant on isotope substitution. More specifically, whereas the classical VER rate constant of

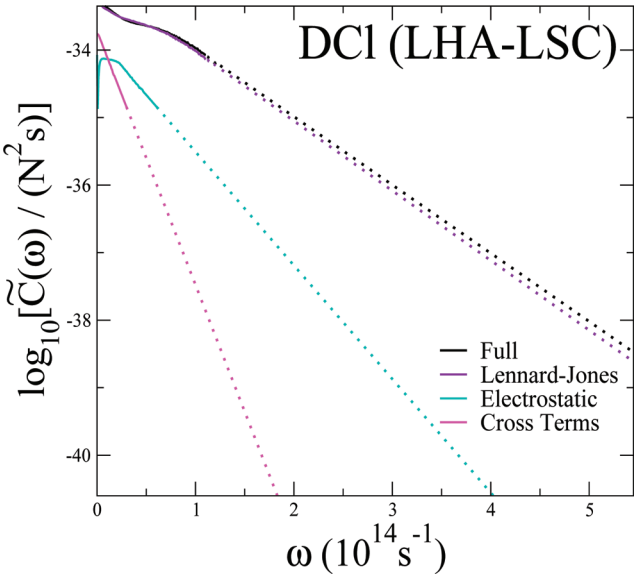

Figure 6. A semilog plot of the LJ−LJ, electrostatic−electrostatic, and LJ−electrostatic cross term contributions to $e^{\beta\hbar\omega/2}\tilde{C}_s^{\mathrm{LHA-LSC}}(\omega)$ for neat DCl (T = 188 K, ρ = 19.671 nm^{-3}).

DCl is faster than that of HCl by a factor of ∼3, the LHA−LSC-based VER rate constant of DCl is slower than that of HCl by a factor of ∼5. Furthermore, the VER rate constant of DCl is seen to be completely dominated by the LJ forces within either classical and LHA−LSC treatments. This should be contrasted with the VER rate constant of HCl, which is dominated by the LJ forces only within the classical treatment. This suggests that VER in HCl and DCl occurs via a different mechanism, namely electrostriction in DCl and quantum delocalization in HCl.

It is interesting to note that a similar argument was recently invoked to explain the isotope effect in the case of H_2/D_2 in liquid Ar.[59] In this case, the experimental VER rate constant of H_2 is about an order of magnitude larger than that of D_2, despite the fact that $\omega_{10}(H_2)$ is larger than $\omega_{10}(D_2)$ by a factor of $\sqrt{2}$. Here too, a classical treatment was unable to account for this trend. However, the LHA−LSC method was able to capture the isotope effect quantitatively, thereby suggesting that its origin is purely quantum-mechanical. More specifically, the smaller mass of H_2 allowed it to penetrate more deeply into classically forbidden regions, thereby sampling stronger repulsive forces, which lead to the enhancement of the VER rate of H_2 relative to that of D_2. The key difference between H_2/D_2 in liquid Ar and liquid HCl/DCl being that the former is a nonpolar system while the latter is polar. Thus, in the case of HCl/DCl, the fact that the Coulombic repulsive wall is actually not as steep as the LJ repulsive wall allows the hydrogen to sample deeper into the region of classically forbidden electrostatic forces, thereby enhancing their contribution relative to that of the LJ forces.

V. SUMMARY

In this paper, we reported the first ever application of the LHA−LSC method to calculating the VER rate constant in a polar liquid. Carrying out this calculation was made easier by the introduction of the force-derivative-free LHA−LSC.[64] The choice of liquid HCl was motivated by the expectation of large quantum effects and the availability of experimental VER rates to compare with. The results indeed confirmed that a classical treatment can be misleading in systems of this type, both quantitatively and qualitatively. From the quantitative point of view, we find that the classical VER rate constant of HCl is 2 orders of magnitude slower than the experimental result. At the same time, the VER rate constant predicted via LHA−LSC was found to be in excellent agreement with experiment. From the qualitative point of view, we found that, while nonpolar forces dominate the classical FFCF, electrostatic forces make a sizable contribution to the FFCF in the case of LHA−LSC. We also found a trend reversal with respect to the effect of isotope substitution on the VER rate constant and underlying mechanism. These results suggest that a classical treatment of VER may not be reliable in predicting VER rates as well as the mechanism underlying them in the case of hydrogen stretches in polar solutions. Further studies on other systems such as CN^-/H_2O[20,41] and HOD/D_2O,[37,92−99] where similar effects can be expected and high-quality experimental data are available, will be necessary in order to establish how general these trends are.

■ ACKNOWLEDGMENT

This project was supported by the National Science Foundation through Grant CHE-0809506.

■ REFERENCES

(1) Faltermeier, B.; Protz, R.; Maier, M. *Chem. Phys.* **1981**, *62*, 377.
(2) Brueck, S. R. J.; Osgood, R. M. *Chem. Phys. Lett.* **1976**, *39*, 568.
(3) Oxtoby, D. W. *Adv. Chem. Phys.* **1981**, *47* (Part 2), 487.
(4) Chateau, M.; Delalande, C.; Frey, R.; Gale, G. M.; Pradère, F. *J. Chem. Phys.* **1979**, *71*, 4799.
(5) Delalande, C.; Gale, G. M. *J. Chem. Phys.* **1979**, *71*, 4804.
(6) Delalande, C.; Gale, G. M. *J. Chem. Phys.* **1980**, *73*, 1918.
(7) Faltermeier, B.; Protz, R.; Maier, M.; Werner, E. *Chem. Phys. Lett.* **1980**, *74*, 425.
(8) Oxtoby, D. W. *Annu. Rev. Phys. Chem.* **1981**, *32*, 77.
(9) Oxtoby, D. W. *J. Phys. Chem.* **1983**, *87*, 3028.
(10) Chesnoy, J.; Gale, G. M. *Ann. Phys. Fr.* **1984**, *9*, 893.
(11) Chesnoy, J.; Gale, G. M. *Adv. Chem. Phys.* **1988**, *70* (part 2), 297.
(12) Harris, C. B.; Smith, D. E.; Russell, D. J. *Chem. Rev.* **1990**, *90*, 481.
(13) Miller, D. W.; Adelman, S. A. *Int. Rev. Phys. Chem.* **1994**, *13*, 359.
(14) Stratt, R. M.; Maroncelli, M. *J. Phys. Chem.* **1996**, *100*, 12981.
(15) Owrutsky, J. C.; Raftery, D.; Hochstrasser, R. M. *Annu. Rev. Phys. Chem.* **1994**, *45*, 519.
(16) Elsaesser, T.; Kaiser, W. *Annu. Rev. Phys. Chem.* **1991**, *42*, 83.
(17) Calaway, W. F.; Ewing, G. E. *J. Chem. Phys.* **1975**, *63*, 2842.
(18) Laubereau, A.; Kaiser, W. *Rev. Mod. Phys.* **1978**, *50*, 607.
(19) Roussignol, P.; Delalande, C.; Gale, G. M. *Chem. Phys.* **1982**, *70*, 319.
(20) Heilweil, E. J.; Doany, F. E.; Moore, R.; Hochstrasser, R. M. *J. Chem. Phys.* **1982**, *76*, 5632.
(21) Heilweil, E. J.; Casassa, M. P.; Cavanagh, R. R.; Stephenson, J. C. *Chem. Phys. Lett.* **1985**, *117*, 185.
(22) Heilweil, E. J.; Casassa, M. P.; Cavanagh, R. R.; Stephenson, J. C. *J. Chem. Phys.* **1986**, *85*, 5004.
(23) Harris, A. L.; Brown, J. K.; Harris, C. B. *Annu. Rev. Phys. Chem.* **1988**, *39*, 341.
(24) Paige, M. E.; Russell, D. J.; Harris, C. B. *J. Chem. Phys.* **1986**, *85*, 3699.
(25) Owrutsky, J. C.; Kim, Y. R.; Li, M.; Sarisky, M. J.; Hochstrasser, R. M. *Chem. Phys. Lett.* **1991**, *184*, 368.
(26) Moustakas, A.; Weitz, E. *J. Chem. Phys.* **1993**, *98*, 6947.

(27) Kliner, D. A. V.; Alfano, J. C.; Barbara, P. F. *J. Chem. Phys.* **1993**, *98*, 5375.
(28) Zimdars, D.; Tokmakoff, A.; Chen, S.; Greenfield, S. R.; Fayer, M. D. *Phys. Rev. Lett.* **1993**, *70*, 2718.
(29) Pugliano, N.; Szarka, A. Z.; Gnanakaran, S.; Hochstrasser, R. M. *J. Chem. Phys.* **1995**, *103*, 6498.
(30) Paige, M. E.; Harris, C. B. *Chem. Phys.* **1990**, *149*, 37.
(31) Salloum, A.; Dubost, H. *Chem. Phys.* **1994**, *189*, 179.
(32) Tokmakoff, A.; Sauter, B.; Fayer, M. D. *J. Chem. Phys.* **1994**, *100*, 9035.
(33) Tokmakoff, A.; Fayer, M. D. *J. Chem. Phys.* **1995**, *103*, 2810.
(34) Urdahl, R. S.; Myers, D. J.; Rector, K. D.; Davis, P. H.; Cherayil, B. J.; Fayer, M. D. *J. Chem. Phys.* **1997**, *107*, 3747.
(35) Owrutsky, J. C.; Li, M.; Locke, B.; Hochstrasser, R. M. *J. Phys. Chem.* **1995**, *99*, 4842.
(36) Laenen, R.; Rauscher, C.; Laubereau, A. *Phys. Rev. Lett.* **1998**, *80*, 2622.
(37) Woutersen, S.; Emmerichs, U.; Nienhuys, H.; Bakker, H. J. *Phys. Rev. Lett.* **1998**, *81*, 1106.
(38) Myers, D. J.; Urdahl, R. S.; Cherayil, B. J.; Fayer, M. D. *J. Chem. Phys.* **1997**, *107*, 9741.
(39) Myers, D. J.; Chen, S.; Shigeiwa, M.; Cherayil, B. J.; Fayer, M. D. *J. Chem. Phys.* **1998**, *109*, 5971.
(40) Sagnella, D. E.; Straub, J. E.; Jackson, T. A.; Lim, M.; Anfinrud, P. A. *Proc. Natl. Acad. Sci. U.S.A.* **1999**, *96*, 14324.
(41) Hamm, P.; Lim, M.; Hochstrasser, R. M. *J. Chem. Phys.* **1997**, *107* (24), 15023.
(42) Lawrence, C. P.; Skinner, J. L. *J. Chem. Phys.* **2002**, *117*, 5827.
(43) Deng, Y.; Stratt, R. M. *J. Chem. Phys.* **2002**, *117*, 1735.
(44) Deng, Y.; Stratt, R. M. *J. Chem. Phys.* **2002**, *117*, 10752.
(45) Sibert, E. L., III; Rey, R. *J. Chem. Phys.* **2002**, *116*, 237.
(46) Li, S.; Thompson, W. H. *J. Chem. Phys.* **2003**, *107*, 8696.
(47) Zwanzig, R. *J. Chem. Phys.* **1961**, *34*, 1931.
(48) Landau, L.; Teller, E. Z. *Z. Sowjetunion* **1936**, *34*, 10.
(49) Mikami, T.; Shigan, M.; Okazaki, S. *J. Chem. Phys.* **2001**, *115*, 9797.
(50) Terashima, T.; Shiga, M.; Okazaki, S. *J. Chem. Phys.* **2001**, *114*, 5663.
(51) Fujisaki, H.; Zhang, Y.; Straub, J. E. *J. Chem. Phys.* **2006**, *124*, 144910.
(52) Leitner, D. M. *Annu. Rev. Phys. Chem.* **2008**, *59*, 233.
(53) Stock, G. *Phys. Rev. Lett.* **2009**, *102*, 118301.
(54) Shi, Q.; Geva, E. *J. Phys. Chem. A* **2003**, *107*, 9059.
(55) Shi, Q.; Geva, E. *J. Phys. Chem. A* **2003**, *107*, 9070.
(56) Ka, B. J.; Shi, Q.; Geva, E. *J. Phys. Chem. A* **2005**, *109*, 5527.
(57) Ka, B. J.; Geva, E. *J. Phys. Chem. A* **2006**, *110*, 9555.
(58) Ka, B. J.; Geva, E. *J. Phys. Chem. A* **2006**, *110*, 13131.
(59) Navrotskaya, I.; Geva, E. *J. Phys. Chem. A* **2007**, *111*, 460.
(60) Shi, Q.; Geva, E. *J. Chem. Phys.* **2003**, *118*, 8173.
(61) Hillery, M.; O'Connell, R. F.; Scully, M. O.; Wigner, E. P. *Phys. Rep.* **1984**, *106* (3), 121.
(62) Berne, B. J.; Thirumalai, D. *Annu. Rev. Phys. Chem.* **1986**, *37*, 401.
(63) Ceperley, D. M. *Rev. Mod. Phys.* **1995**, *67*, 279.
(64) Vazquez, F. X.; Navrotskaya, I.; Geva, E. *J. Phys. Chem. A* **2010**, *114*, 5682.
(65) Legay-Sommaire, N.; Legay, F. *Chem. Phys.* **1977**, *52*, 213.
(66) Chesnoy, J.; Richard, D. *Chem. Phys.* **1982**, *67*, 347.
(67) Chesnoy, J.; Richard, D. *Chem. Phys. Lett.* **1982**, *92*, 449.
(68) Whitnell, R. M.; Wilson, K. R.; Hynes, J. T. *J. Phys. Chem.* **1990**, *94*, 8625.
(69) Whitnell, R. M.; Wilson, K. R.; Hynes, J. T. *J. Chem. Phys.* **1992**, *96*, 5354.
(70) Benjamin, I.; Whitnell, R. M. *Chem. Phys. Lett.* **1993**, *204*, 45.
(71) Bruehl, M.; Hynes, J. T. *Chem. Phys.* **1993**, *175*, 205.
(72) Gnanakaran, S.; Hochstrasser, R. M. *J. Chem. Phys.* **1996**, *105*, 3486.
(73) Chorny, I.; Vieceli, J.; Benjamin, I. *J. Chem. Phys.* **2002**, *116*, 8904.
(74) Rey, R.; Hynes, J. T. *J. Chem. Phys.* **1996**, *104*, 2356.
(75) Lawrence, C. P.; Skinner, J. L. *J. Chem. Phys.* **2003**, *118*, 264.
(76) Ferrario, M.; Klein, M. L.; McDonald, I. R. *Chem. Phys. Lett.* **1993**, *213*, 537.
(77) Morita, A.; Kato, S. *J. Chem. Phys.* **1998**, *109*, 5511.
(78) Rey, R.; Hynes, J. T. *J. Chem. Phys.* **1998**, *108*, 142.
(79) Gulmen, T. S.; Sibert, E. L., III *J. Phys. Chem. A* **2004**, *108*, 2389.
(80) Gulmen, T. S.; Sibert, E. L., III *J. Phys. Chem. A* **2005**, *109*, 5777–5780.
(81) Laage, D.; Demirdjian, H.; Hynes, J. T. *Chem. Phys. Lett.* **2005**, *405*, 453.
(82) Skinner, J. L.; Park, K. *J. Phys. Chem. B* **2001**, *105*, 6716.
(83) Chorny, I.; Benjamin, I. *J. Mol. Liq.* **2004**, *110*, 133.
(84) Vieceli, J.; Chorny, I.; Benjamin, I. *J. Chem. Phys.* **2002**, *117*, 4532.
(85) Ladanyi, B. M.; Stratt, R. M. *J. Chem. Phys.* **1999**, *111*, 2008.
(86) Lim, M.; Gnanakaran, S.; Hochstrasser, R. M. *J. Chem. Phys.* **1997**, *106*, 3485.
(87) Schofield, P. *Phys. Rev. Lett.* **1960**, *4*, 239.
(88) Wang, J.; Wolf, R. M.; Caldwell, J. W.; Kollamn, P. A.; Case, D. A. *J. Comput. Chem.* **2004**, *25*, 1157.
(89) Nitzan, A.; Mukamel, S.; Jortner, J. *J. Chem. Phys.* **1974**, *60*, 3929.
(90) Nitzan, A.; Mukamel, S.; Jortner, J. *J. Chem. Phys.* **1975**, *63*, 200.
(91) Rostkier-Edelstein, D.; Graf, P.; Nitzan, A. *J. Chem. Phys.* **1997**, *107*, 10470.
(92) Graener, H.; Seifert, G.; Laubereau, A. *Phys. Rev. Lett.* **1991**, *66*, 2092.
(93) Vodopyanov, K. L. *J. Chem. Phys.* **1991**, *94*, 5389.
(94) Nienhuys, H.; Woutersen, S.; van Santen, R. A.; Bakker, H. J. *J. Chem. Phys.* **1999**, *111*, 1494.
(95) Deak, J. C.; Rhea, S. T.; Iwaki, L. K.; Dlott, D. D. *J. Phys. Chem. A* **2000**, *104*, 4866.
(96) Rey, R.; Hynes, J. T. *Chem. Rev.* **2004**, *104*, 1915.
(97) Wang, Z.; Pakoulev, A.; Pang, Y.; Dlott, D. D. *Chem. Phys. Lett.* **2003**, *378*, 281.
(98) Pakoulev, A.; Wang, Z.; Dlott, D. D. *Chem. Phys. Lett.* **2003**, *371*, 2203.
(99) Pakoulev, A.; Wang, Z.; Pang, Y.; Dlott, D. D. *Chem. Phys. Lett.* **2003**, *380*, 404.